Tunable threshold voltage and flatband voltage in pentacene field effect transistors

Annie Wang,[a] Ioannis Kymissis,[b] Vladimir Bulović, and Akintunde I. Akinwande
Microsystems Technology Laboratory, Massachusetts Institute of Technology, Cambridge, Massachusetts 02139

(Received 19 April 2006; accepted 17 July 2006; published online 12 September 2006)

Charged interface states are introduced by UV-ozone treatment of a polymer gate dielectric, parylene, prior to deposition of the organic semiconductor, pentacene, thereby modifying the organic field effect transistor (OFET) operation from enhancement to depletion mode. Quasistatic capacitance-voltage measurements and the corresponding current-voltage characteristics show that the threshold voltage V_T and flatband voltage V_{FB} can be shifted by over +50 V, depending on the ozone exposure time. This work demonstrates that careful control of the semiconductor-insulator interface state densities is essential to V_T and V_{FB} control and the fabrication of reliable OFET integrated circuits. © *2006 American Institute of Physics*. [DOI: 10.1063/1.2349299]

Chemical properties of the interface between the gate dielectric and the organic semiconductor of organic field effect transistors (OFETs) can influence the charged carrier transport in the semiconducting channel[1–3] and affect OFET threshold voltage V_T and flatband voltage V_{FB}.[4–6] The ability to fabricate OFETs with reproducible and tunable V_T and V_{FB} is critical for practical circuit design, improved circuit functionality and yield, and motivates the present study, which considers a method for tuning V_T and V_{FB} and applies it to pentacene OFETs.

Much of the literature on OFETs derives the value of V_T from OFET conduction measurements,[7,8] which are generally affected by distorting factors such as charge trapping at semiconductor defects, source/drain contact resistance, and gate-bias-dependent effective carrier mobilities. Also, unlike conventional silicon metal-oxide-semiconductor (MOS) FETs, most OFETs operate as accumulation mode devices, with V_{FB}, obtained from quasi-static capacitance-voltage (C-V) measurements[9] and defined as the gate bias at which charge appears in the channel, analogous to the threshold voltage in inversion mode silicon MOSFETs.[10] As the magnitude of the gate bias increases, charge first accumulates in the trap states of the OFET channel and contacts. Consequently, the induced charges are not immediately available for conduction.[11] This results in different values for the C-V-derived V_{FB} and the current-voltage-derived V_T, but the two values are related, as we demonstrate in this study.

We report the results from a process-level technique for modifying V_T and V_{FB} of pentacene OFETs using a timed UV-ozone treatment of an organic gate dielectric, parylene, prior to pentacene deposition. This approach introduces charged states at the semiconductor-dielectric interface that result in a shift of V_{FB} and the consequent shift of V_T. Other process techniques, such as O_2 plasma treatment of the dielectric, can also be used to rapidly shift V_T by over +100 V in just a 5 s exposure.[12] In contrast, UV-ozone treatment is a more gradual method of adjusting V_T. Quasistatic capacitance-voltage measurements and current-voltage characteristics demonstrate that with increasing lengths of UV-ozone exposure, V_T and V_{FB} are shifted gradually and the magnitude of $|V_{FB}-V_T|$ increases.

Pentacene field effect transistors were fabricated on glass substrates using an organic polymer, parylene-C, as the gate dielectric. Yasuda *et al.* reported that among the several varieties of parylene available, parylene-C resulted in FETs with the highest field effect mobility and on/off current ratio.[13] Parylene is deposited at room temperature in a chemical vapor deposition process in which parylene is fully reacted, requiring no additional process steps.

Patterning of the aluminum gates, pentacene layer, and gold source/drain contacts was performed using shadow masks, resulting in the bottom-gate, top-contact devices of Fig. 1(a). Parylene was deposited by hot filament chemical vapor deposition over the patterned gates. For all devices except the control devices, the parylene dielectric was treated in UV ozone. In the first set of devices (data of Fig. 2), the parylene layer was 320 nm thick and UV-ozone exposure times ranged from 12 s to 1 min. In the second set of devices (data of Fig. 3), the parylene layer was 190 nm thick and exposure times ranged from 30 s to 5 min. A 10 nm layer of pentacene was then thermally evaporated at a rate of 0.01 nm/s onto the parylene in a 1×10^{-6} Torr vacuum chamber. Finally, patterned gold source/drain contacts were deposited by electron beam deposition. The fabricated OFETs [Fig. 1(b)] have a channel length of 50 μm and a channel width of 1250 μm.

Electrical characterization of the pentacene FETs was performed on an Agilent 4156C semiconductor parameter analyzer. Quasistatic capacitance-voltage (C-V) curves were obtained by setting the source and drain bias at 0 V and

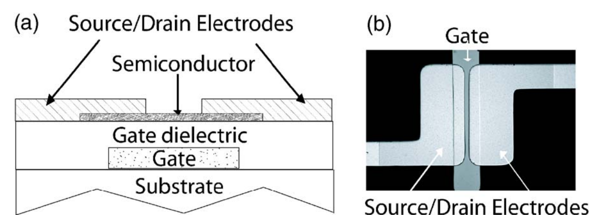

FIG. 1. (Color online) OFET device structure. (a) Schematic cross section of bottom-gate, top-contact OFET device. (b) Photograph of the OFET. The channel dimensions are $W/L=1250\ \mu$m/50 μm.

[a]Electronic mail: aiwang@mit.edu
[b]Electronic mail: johnkym@alum.mit.edu

 © 2006 American Institute of Physics
Downloaded 03 Feb 2007 to 18.51.1.222. Redistribution subject to AIP license or copyright, see http://apl.aip.org/apl/copyright.jsp

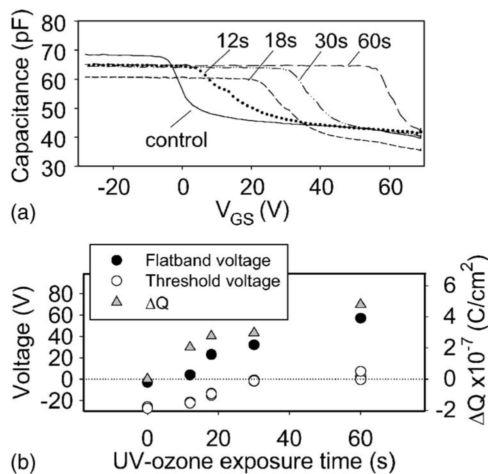

FIG. 2. (a) Quasistatic C-V measurement of control and UV-ozone treated devices, with the UV-ozone exposure time indicated in the figure. Flatband voltage becomes more positive as UV-ozone exposure time increases. (b) Threshold voltage and flatband voltage (left axis) and increase in charge density ΔQ (right axis) as a function of UV-ozone exposure time. V_T is calculated in the linear region, $V_{DS}=-4$ V. Three different devices from each sample were characterized and plotted. The parylene thickness is 320 nm.

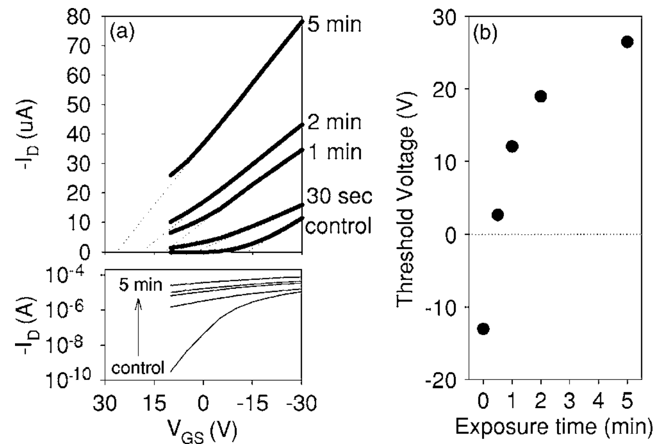

FIG. 3. (a) V_{GS} sweep and V_T extrapolation for UV-ozone treated devices, where $V_{DS}=-4$ V (top). $I_{DS}-V_{GS}$ characteristic on semilog plot (bottom). (b) V_T extrapolated from the linear region fit of (a) as a function of UV-ozone exposure time. The parylene thickness is 190 nm.

sweeping the gate bias, V_{GS}. Current-voltage (I-V) curves were obtained by sweeping the drain-to-source voltage V_{DS} at different V_{GS}, or by setting V_{DS} and sweeping V_{GS} to obtain transfer characteristics.

The quasistatic C-V curves in Fig. 2(a) show that V_{FB}, obtained as in Ref. 9, shifts more positive with UV-ozone treatment and increases monotonically with exposure time. In the first set of devices, V_{FB} shifted by more than +50 V from the control to the 60 s treated device while the parylene capacitance C_{ins} measured on an independent Al/parylene/Au sandwich structure remained at 9 nF/cm^2. The ~25 pF modulation in the capacitance value between the accumulation ($V_{GS}<V_{FB}$) and depletion ($V_{GS}>V_{FB}$) regions of the C-V traces reflects the charging of both the $1250\times 50\ \mu\text{m}^2$ pentacene channel and an additional $750\times 300\ \mu\text{m}^2$ pentacene area that is outside the channel but still over the gate metal and in contact with the source/drain contacts. Variation in the shadow mask alignment across the sets of devices caused the difference in the overlap capacitances of gate and source/drain contacts for each device set. This is reflected in the OFET accumulation capacitance offsets at $V_{GS}=-25$ V and does not affect V_{FB}.

We quantify the increase in the interface charge density with ozone treatment by integrating the area under the C-V curves of the control and each of the treated devices, $\Delta Q=\int(C_t-C_c)dV$. Here C_t and C_c correspond to the capacitances of the treated and control devices, respectively, adjusted for the offsets due to different overlap capacitances. The values of ΔQ are on the order of 10^{-7} C/cm^2, or 10^{12} charges/cm^2, and are plotted in Fig. 2(b) together with V_{FB} and V_T, the derivation of which is discussed below.

Current-voltage characteristics (solid line) and V_T extrapolation (dashed line) for the second set of devices are plotted in Fig. 3(a) (top). V_T was determined by fitting a straight line to the I_{DS}-V_{GS} plot and extrapolating to $I_D=0$. Although V_T is usually defined as V_{GSi}-$V_{DS}/2$, where V_{GSi} is the intercept gate voltage,[14] here we have defined V_T as V_{GSi} and neglected the $V_{DS}/2$ constant. The corresponding V_T plot is shown in Fig. 3(b). V_T was measured in the OFET linear region at a low drain-to-source bias ($V_{DS}=-4$ V) to maintain a uniform lateral electric field in the channel. V_T increased monotonically with UV-ozone exposure time, shifting from −13 V in the control up to +26 V in the treated devices. The shift in V_T and the increased conductivity in the treated devices over the range of V_{GS} shown in Fig. 3(a) can be explained by the presence of additional positive mobile charges in the channel after the UV-ozone treatment.

Higher subthreshold slopes S are consistent with an increasing interface state density. While S was only calculated for the control device ($S=4.7$ V/decade) because the parylene dielectric breaks down before the treated devices fully turn off, Fig. 3(a) (bottom) shows that the on/off ratio decreases and subthreshold slope increases with ozone treatment. In contrast, the field effect mobility μ calculated as in Ref. 8 from the I_{DS}-V_{GS} plot in Fig. 3(a) (top) does not change significantly: $\mu=0.41$, 0.23, 0.46, 0.48, and 0.71 cm^2/V s in the control, 30 s, 1 min, 2 min, and 5 min treated devices, respectively. Since the calculation of μ from conduction measurements suffers from ambiguities similar to those in the extraction of V_T, an alternative method suggested in Ref. 15 can also be used to determine μ and show that μ does not change significantly.

In the first device set, V_T shifted from −27 V in the control up to +7 V in the treated devices. Note that because of a thicker gate dielectric, the V_T magnitude of the control device, shown in Fig. 2, is larger than that shown in Fig. 3. The monotonic increase in V_T is consistent with the monotonic increase in V_{FB} with an offset of up to 47 V.

To explain the observed results, we suggest that the UV ozone chemically reacts with the parylene surface, generating fixed charged sites, with density Q_{fixed}, that electrostatically attract carriers in the overlying pentacene. More charged sites are generated at the surface of the dielectric as the exposure time is increased. This is reflected in the increasing offset between V_T and V_{FB}. V_T is a measure of the onset of conduction and of the presence of mobile charges Q_{mobile} in the channel. In contrast, V_{FB} depends on the total number of charges, $Q_{mobile}+Q_{fixed}$, at the semiconductor-dielectric interface. The increasing V_T-V_{FB} offset with the increasing UV-ozone exposure is, therefore, due to the in-

Downloaded 03 Feb 2007 to 18.51.1.222. Redistribution subject to AIP license or copyright, see http://apl.aip.org/apl/copyright.jsp

crease in Q_{fixed}. A detailed model for the I_D dependence as a function of fixed and mobile charge concentrations in the FET linear region is developed in Ref. 12. The positive shifts in V_{FB} and V_T indicate that the charged sites are negative, inducing positive mobile charges that increase pentacene conductivity. A larger Q_{fixed} results in a larger V_T shift, suggesting that V_T can be controlled and reproduced by carefully modifying Q_{fixed}, whether by UV-ozone treatment or another process technique.

We demonstrated that quasistatic *C-V* is a useful diagnostic tool for studying carrier concentrations in the channel since V_{FB} can be determined directly from the *C-V* characteristic, without the ambiguity in the model-based extrapolation of V_T from *I-V* characteristics. Still, V_T is useful as an indicator of when carriers in the channel contribute to conduction, necessitating both measurement methods for a full evaluation of OFET performance.

We applied *C-V* and *I-V* measurements on a series of OFET devices in order to systematically evaluate the influence of the trapped charge at the semiconductor-dielectric interface. For each OFET we modified threshold voltage at the process level by using an UV-ozone treatment to introduce charged states on the gate dielectric surface prior to pentacene deposition. Electrical characterization shows that flatband and threshold voltage can be increased monotonically depending on the UV-ozone exposure time. These results demonstrate that careful control of semiconductor-dielectric interface states is essential to controlling V_T and V_{FB} in OFETs.

This research is sponsored by the U.S. Army Natick Center and the MARCO Focus Center for Materials, Structures, and Devices.

[1] T. W. Kelley, L. D. Boardman, T. D. Dunbar, D. V. Muyres, M. J. Pellerite, and T. P. Smith, J. Phys. Chem. B **107**, 5877 (2003).
[2] H. Klauk, M. Halik, U. Zschieschang, G. Schmid, and W. Radlik, J. Appl. Phys. **92**, 5259 (2002).
[3] D. J. Gundlach, C.-C. Kuo, C. D. Sheraw, J. A. Nichols, and T. N. Jackson, Proc. SPIE 4466, 54 (2001).
[4] J. Lee, J. H. Kim, and S. Im, J. Appl. Phys. **96**, 2301 (2004).
[5] S. Kobayashi, T. Nishikawa, T. Takenobu, S. Mori, T. Shimoda, T. Mitani, H. Shimotani, N. Yoshimoto, S. Ogawa, and Y. Iwasa, Nat. Mater. **3**, 317 (2004).
[6] K. P. Pernstich, S. Haas, D. Oberhoff, C. Goldmann, D. J. Gundlach, B. Batlogg, A. N. Rashid, and G. Schitter, J. Appl. Phys. **96**, 6431 (2004).
[7] G. Horowitz, X. Peng, D. Fichou, and F. Garnier, J. Appl. Phys. **67**, 528 (1990).
[8] *1620 IEEE Standard for Test Methods for the Characterization of Organic Transistors and Materials* (IEEE Std., New York, 2004), pp. 1–12.
[9] D. K. Schroder, *Semiconductor Material and Device Characterization* (Wiley-Interscience, New York, 1998), p. 350.
[10] E. J. Meijer, C. Tanase, P. W. M. Blom, E. van Veenendaal, B.-H. Huisman, D. M. de Leeuw, and T. M. Klapwijk, Appl. Phys. Lett. **80**, 3838 (2002).
[11] M. Jacunski, M. Shur, and M. Hack, IEEE Trans. Electron Devices **43**, 1433 (1996).
[12] A. Wang, I. Kymissis, V. Bulovic, and A. I. Akinwande, IEEE Trans. Electron Devices **53**, 9 (2006).
[13] T. Yasuda, K. Fujita, H. Nakashima, and T. Tsutsui, Jpn. J. Appl. Phys., Part 1 **42**, 6614 (2003).
[14] D. K. Schroder, *Semiconductor Material and Device Characterization* (Wiley-Interscience, New York, 1998), p. 243.
[15] K. Ryu, I. Kymissis, V. Bulovic, and C. G. Sodini, IEEE Electron Device Lett. **26**, 716 (2005).

Downloaded 03 Feb 2007 to 18.51.1.222. Redistribution subject to AIP license or copyright, see http://apl.aip.org/apl/copyright.jsp